THE DESIGN AND OPERATION OF A SLOW NEUTRON CHOPPER

by

Roland George Struss

A Thesis Submitted to the
Graduate Faculty in Partial Fulfillment of
The Requirements for the Degree of
MASTER OF SCIENCE

Major Subject: Nuclear Engineering

Iowa State University
Of Science and Technology
Ames, Iowa

1966

TABLE OF CONTENTS

INTRODUCTION

The utilization of nuclear research reactors often involves experiments which require the separation of neutrons by their velocities. A neutron chopper is designed to allow the separation of neutrons of different velocities by a time of flight technique. A slow neutron chopper is a device that interrupts or "chops" a beam of low energy neutrons to produce pulses of slow neutrons. These pulses are then allowed to spread out over a given flight path which provides separation of the neutrons by velocity. Suitable counting techniques are employed to count the number of neutrons in a discrete velocity range at successive time intervals after burst transmission.

The energy dependence of the neutron absorption cross section of boron was measured in the early 1940's by Fermi and his colleagues using the first slow neutron chopper (2). Since that time many measurements have been made with devices of this type, and several styles of choppers have been devised.

A slow neutron chopper designed for maximum energy range as well as for great flexibility in operation is described. Discussions of theoretical factors affecting the design and the physical design details are presented. A description of the fabrication and operation of this slow neutron chopper is

given with both theoretical and practical details. The results presented were obtained in the initial operation. They define the spectrum of thermal neutrons in the graphite thermal column of the Ames Laboratory Research Reactor.

The successful operation of this device validates the design and fabrication details, producing a chopper which can be used in various experimental measurements. Some possible applications and measurements are discussed in the conclusion of the thesis.

REVIEW OF LITERATURE

A number of slow neutron choppers utilizing similar principles of operation have been described in the literature. The general principles involved in the design of these choppers are presented to provide a basis of comparison.

The machines built early in the nuclear era employed a revolving cylinder of laminated construction. The laminae were composed of alternate layers of materials that absorb and transmit neutrons in the energy region of interest. Devices of this type are described by Fermi, Marshall, and Marshall (2) and by Egelstaff (1).

The common feature of this type of neutron chopper is the constantly varying length of the transmitting slits due to cylinder curvature. The machines can be driven at different rotational speeds to change the energy range, but it is difficult to change the laminated structure unless the entire rotor is replaced. This limited the experimenters to one neutron absorbing material and a fixed transmitting slit thickness.

Another method of mounting the laminated structure of absorbing and transmitting materials is suggested in articles by Hoch (4) and by Mastovoi, Pevzner and Tsitovich (7). The axis of the sandwich construction in these designs is mounted

at right angles to the rotor axis. This arrangement eliminates the large variation in the slit length due to rotor curvature. It is further suggested by Hoch that the sandwich assembly could be designed as a moveable carrier. This could allow a variation in the transmitting slit thickness and easy replacement of the entire laminated structure.

Egelstaff presents a detailed discussion of operation of a slow neutron chopper. A thorough discussion of the parameters that affect the operation of a chopper is followed by actual results of measurements made at the facilities in Harwell, England. The literature studied by this author has not presented the details of variation in chopper transmission with velocity. These will be discussed at some length in this thesis. Other authors used previously developed transmission functions, which are not derived in the original references.

A document describing some typical experiments and measurements at the Argonne Laboratory has been an excellent general reference (9). The document is published as a part of the Reactor Laboratory Experiments for the International Institute of Nuclear Science and Engineering. The general discussions of theory and operational procedures are based on the Fermi slow neutron chopper used at Argonne.

DISCUSSION OF THEORY

The theory regarding slow neutron choppers has been developed by others (1,2,7) and will be discussed here as it pertains to chopper operation. A schematic diagram of a slow neutron chopper is shown in Figure 1 with the same legend that is used in this discussion. The shutter which produces the pulses of neutrons is composed of cadmium absorber plates separated by a material such as aluminum that readily transmits neutrons. This shutter has the beam interrupted most of the time during rotor rotation, with neutrons being transmitted twice per revolution while the aluminum separators are parallel to the neutron beam. The aluminum slits are open for approximately one degree of rotation, dependent on the transmitting material thickness. This produces the pulses or bursts of neutrons which are separated sufficiently in time to allow the neutrons to spread out along the flight path by their velocity differences.

A counting circuit is started by a signal generated during rotor rotation, and a gate circuit allows the counting of neutrons arriving at the detector in the fixed time interval of the gate. The neutrons counted in this set time interval then represent those having a small range of velocities

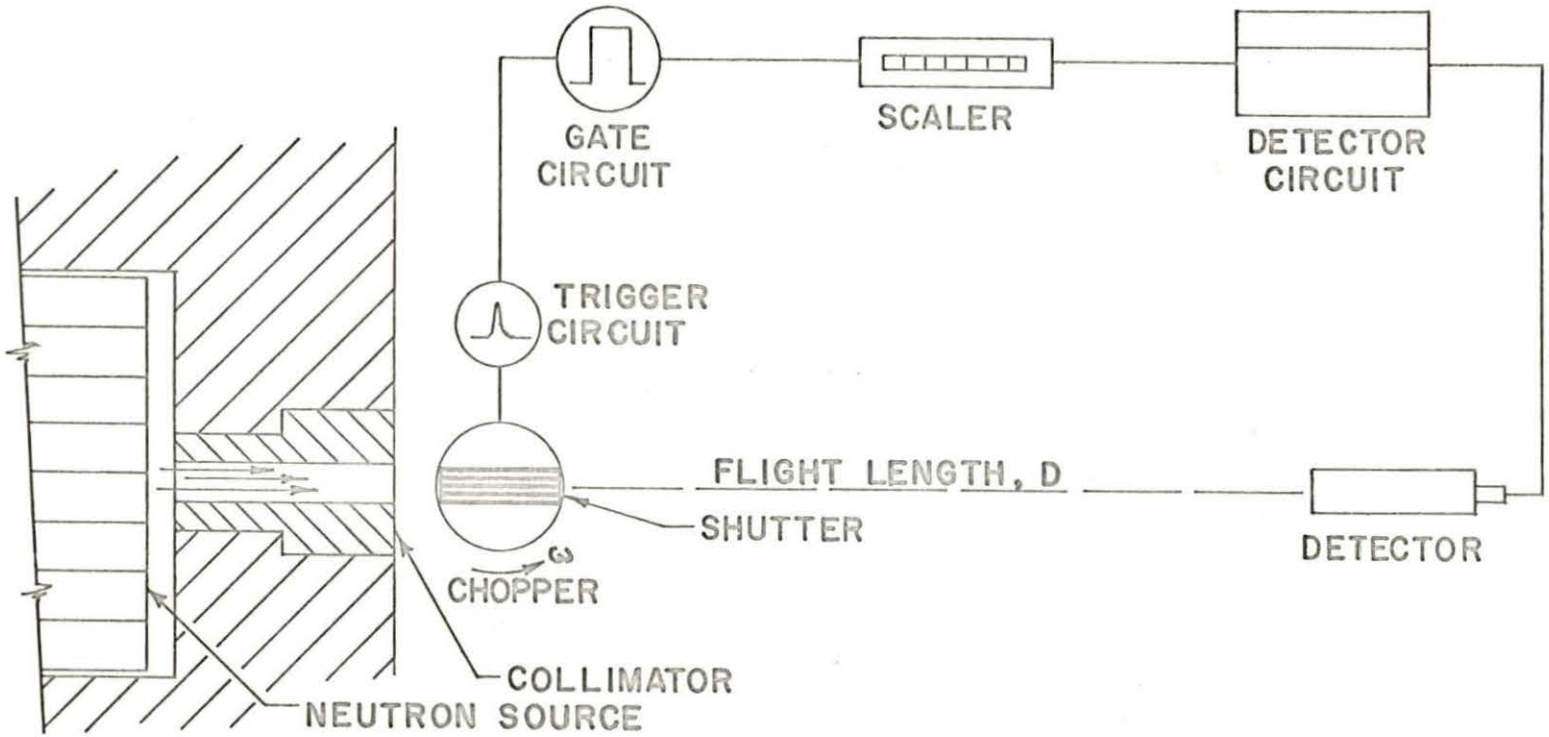

Figure 1. Block diagram of chopper setup

defined by the ratio of flight length and time of flight.

The essential equations defining these operation parameters are given with a detailed discussion of the aperture function. The nomenclature and symbols used are the same as those generally found in the literature. All the equations except the aperture function are available in the references cited at the beginning of this section.

The shutter is driven with a rotation speed of ω radians per second. The straight line transmission through the shutter is then by geometry, of duration T_n, produced twice per revolution so

$$T_n = \frac{S}{\omega R}$$

where S is the slit width and R is 1/2 the slit length.

The transmission of neutrons that are too slow to traverse the straight line opening, $v \leq 2\omega R^2/S$, is given later by the aperture function. The neutrons that cannot traverse the length of the slit during the time it is open are simply cut off by the absorber plates. This velocity, v_{co}, is

$$v_{co} = \frac{\omega R^2}{S} .$$

This shows that all neutrons having a velocity greater than the cutoff velocity are transmitted by the chopper when the shutter is open. The consideration of how these neutrons

are transmitted by a revolving slit gives the aperture function. It is assumed that a collimated parallel beam of neutrons is incident on the rotating shutter, which is opening and closing as shown in Figure 2. The function describes the transmission for the central slit, but the transmission of any slit is given when the speed of opening and closing includes the cosine function for the velocity of the ends of the slit. The effect of this consideration on the aperture function has been neglected to simplify the illustration. A scale layout of the outermost slit shows this error to be much less than one percent.

Referring to Figure 2, area A_1 is bounded by

$$x_1(t) \leq x \leq \frac{S}{2} ; \quad 0 \leq t \leq \frac{S}{\omega R}$$

$$-\frac{S}{2} \leq x \leq x_2(t); \quad \frac{S}{\omega R} \leq t \leq \frac{2S}{\omega R}$$

and by geometry it is seen that

$$x_1(t) = \frac{S}{2} - \omega R t$$

$$x_2(t) = x_1(t) + S$$

so that A_1 is bounded by

$$\frac{S}{2} - \omega R t \leq x \leq \frac{S}{2} ; \quad 0 \leq t \leq \frac{S}{\omega R}$$

$$-\frac{S}{2} \leq x \leq \frac{3S}{2} - \omega R t; \quad \frac{S}{\omega R} \leq t \leq \frac{2S}{\omega R}$$

and it can be shown also that A_2 is bounded by

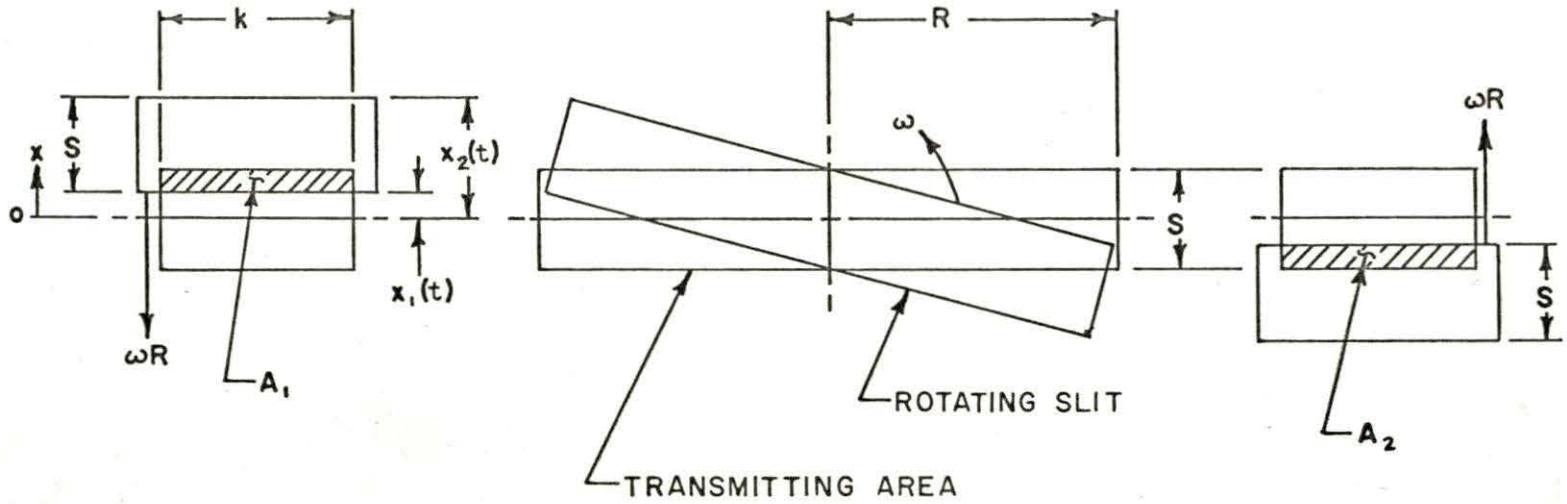

Figure 2. Representation of slit opening and closing

$$-\frac{S}{2} \leq x \leq \omega Rt - \frac{S}{2} \; ; \quad 0 \leq t \leq \frac{S}{\omega R}$$

$$\omega Rt - \frac{3S}{2} \leq x \leq \frac{S}{2} \; ; \quad \frac{S}{\omega R} \leq t \leq \frac{2S}{\omega R}$$

The foregoing is based on time equal to zero at the start of the area formation. Because the neutron transmission is a function of time and space, the time base will be moved to the center of the slit, and the aperture function will be symmetric in time. This can be shown by delaying $A_1(t)$ by time R/v to get $A_1(t - R/v)$ bounded by

$$\frac{S}{2} - \omega R(t - \frac{R}{v}) \leq x \leq \frac{S}{2} \; ; \quad \frac{R}{v} \leq t \leq \frac{S}{\omega R} + \frac{R}{v}$$

$$-\frac{S}{2} \leq x \leq \frac{3S}{2} - \omega R(t - \frac{R}{v}) \; ; \quad \frac{S}{\omega R} + \frac{R}{v} \leq t \leq \frac{2S}{\omega R} + \frac{R}{v}$$

and advancing $A_2(t)$ by time R/v gives $A_2(t + R/v)$ bounded by

$$-\frac{S}{2} \leq x \leq \omega R(t + \frac{R}{v}) - \frac{S}{2} \; ; \quad -\frac{R}{v} \leq t \leq \frac{S}{\omega R} - \frac{R}{v}$$

$$\omega R(t + \frac{R}{v}) - \frac{3S}{2} \leq x \leq \frac{S}{2}; \quad \frac{S}{\omega R} - \frac{R}{v} \leq t \leq \frac{2S}{\omega R} - \frac{R}{v} \; .$$

The curves representing these boundaries are shown in Figure 3. The points of intersection have been found by simultaneous solution of the equations of the lines connecting the curves. The transmission of neutrons of any given velocity is represented by the area bounded by the four hyperbolic curves. It can be seen that the trans-

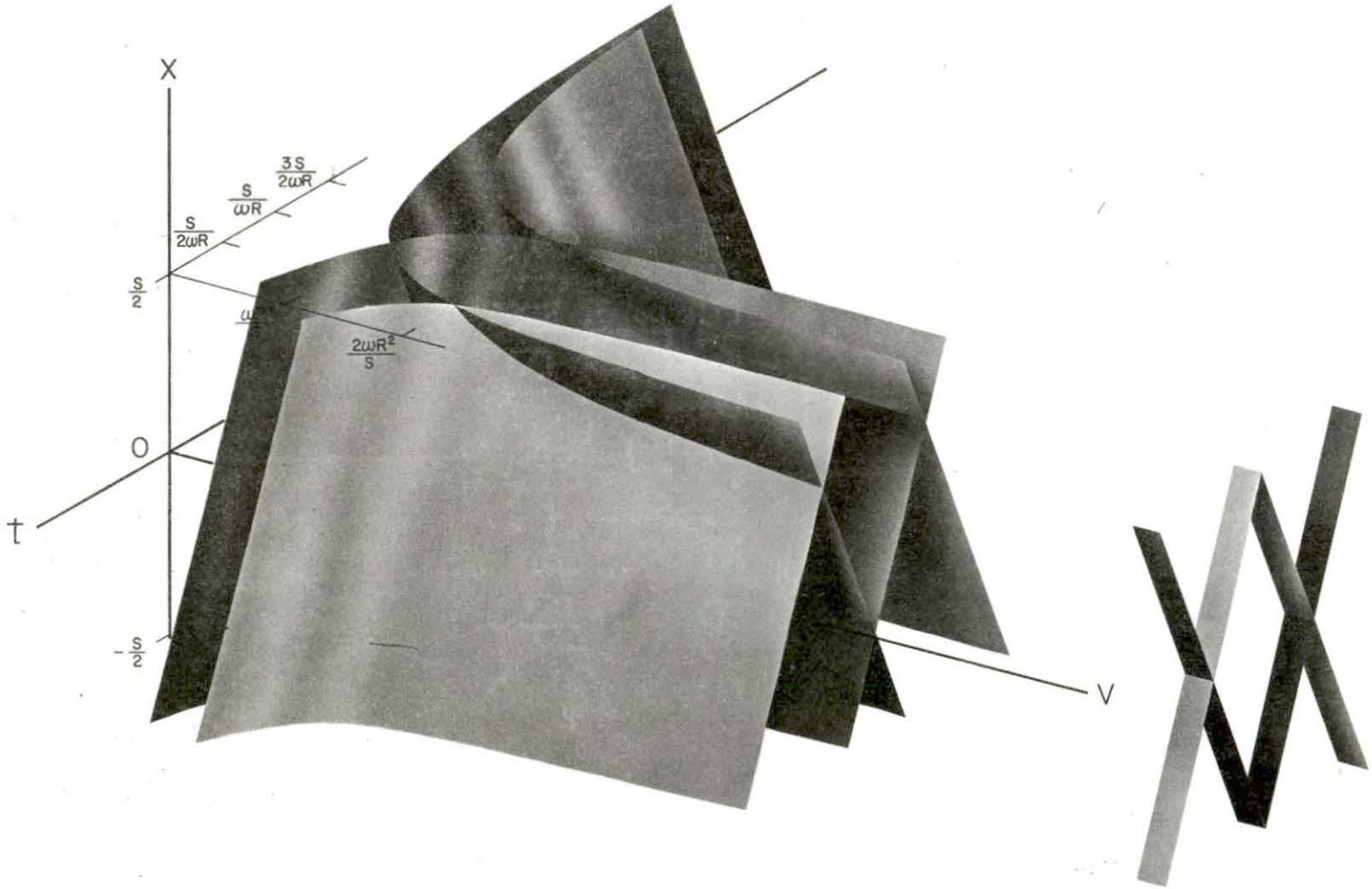

Figure 3. Graphical illustration of aperture function

mission of neutrons at the cutoff velocity is zero. Figure 3 thus shows graphically the transmission of neutrons of various velocities versus time. This figure is then used to develop a set of figures and equations which describe the transmission of the chopper. The time base zero can be shifted to the time when the chopper is fully open. The composite curves describing these burst shapes are shown in Figure 4. The transmission is divided into four regions to describe the chopper transmission mathematically.

The separate aperture functions A(v,t) are given for the four regions by

$$A_1(v,t) = 2\omega Rt - S \; ; \quad \frac{S}{2\omega R} \leq t \leq \frac{S}{\omega R} - \frac{R}{v}$$

$$v \geq \frac{2\omega R^2}{S}$$

$$A_2(v,t) = \omega Rt - \frac{\omega R^2}{v} \; ; \quad \frac{S}{\omega R} - \frac{R}{v} \leq t \leq \frac{S}{\omega R}$$

$$v \geq \frac{\omega R^2}{S}$$

$$A_3(v,t) = 2S - \omega Rt - \frac{\omega R^2}{v} \; ; \quad \frac{S}{\omega R} \leq t \leq \frac{S}{\omega R} + \frac{R}{v}$$

$$v \geq \frac{\omega R^2}{S}$$

$$A_4(v,t) = 3S - 2\omega Rt \; ; \quad \frac{R}{v} + \frac{S}{\omega R} \leq t \leq \frac{3S}{2\omega R}$$

$$v \geq \frac{2\omega R^2}{S} \; .$$

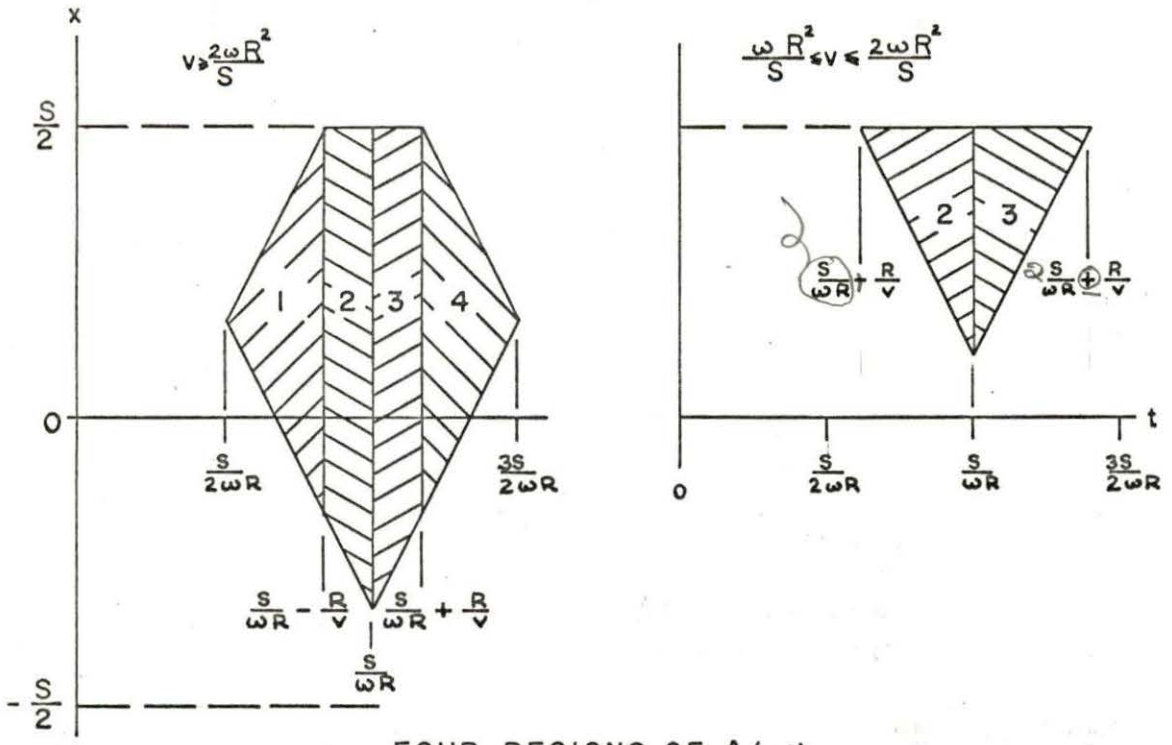

FOUR REGIONS OF A(v,t)

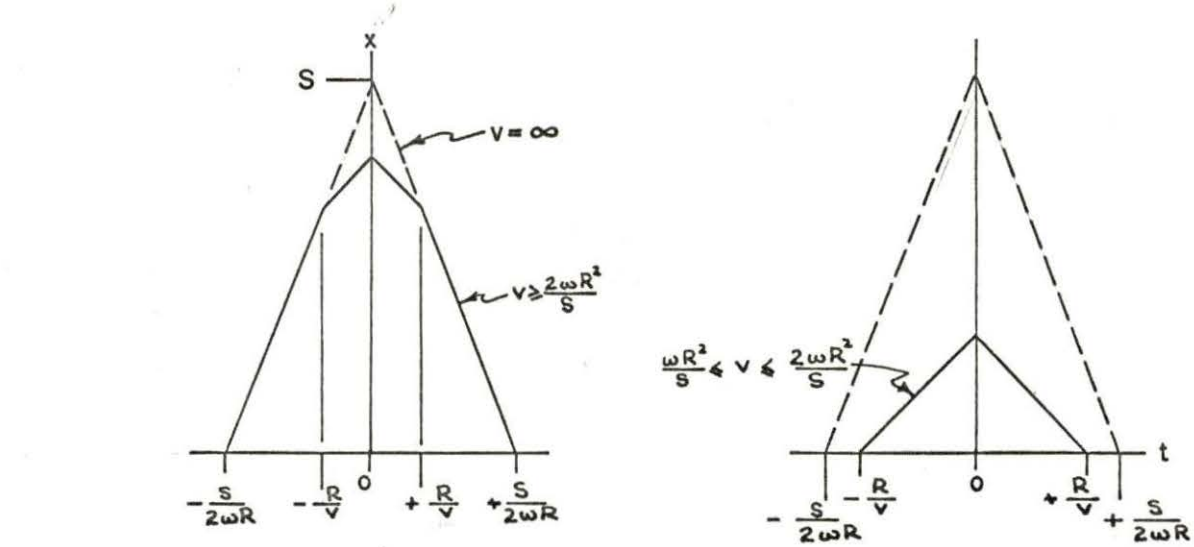

F(v,t) - SHIFTED IN TIME

Figure 4. Composite curves of burst shapes

The addition of the separate aperture functions gives F(v,t) which describes the modulation of the neutron spectrum by the chopper in time and velocity. This is represented by

$$F(v,t) = N(v)\ A(v,t)$$

where N(v) is the number of neutrons of velocity v, and A(v,t) is the transmission of neutrons defined by the separate aperture functions.

This development of the aperture function is intended to describe the existence of neutrons in space and time as they travel through the chopper and then on to the detector. This function is not developed in the literature, and it is required to relate the neutrons which get counted to the total number of neutrons of velocity v in the incident beam.

The aperture function is used to provide the correlation back to the original velocity spectrum by considering the maximum aperture function as the one for neutrons with infinite velocities. All other functions for slower neutrons will then be some fraction of the infinite velocity function, and the correction factor, f(x), is then defined as

$$f(x) = \frac{A(v,t)}{A(v_\infty,t)} \ .$$

The width of the slit should be considered as well as the height to get a proper transmission function. This width is

denoted as the constant k in Figure 2. Then for region one at the chopper

$$A_1(v,t) = k(2\omega Rt - S).$$

A(v,t) is maximum when $v = \infty$, and from Figure 4 the maximum height is at $t = S/\omega R$. Using these values to solve for the constant k and setting

$$A_{max} = kS$$

then

$$k = \frac{A_{max}}{S} .$$

Geometric inspection of Figure 4, shows that the area of the burst for infinite velocity neutrons is

$$A(v_\infty,t) = \tfrac{1}{2} \frac{S^2}{\omega R} k$$

or

$$A(v_\infty,t) = A_{max} \frac{S}{2\omega R} .$$

For neutrons with velocities between $2\omega R^2/S$ and infinity,

$$A(v,t) = [A_1 + A_2 + A_3 + A_4](v,t).$$

Summing these areas by geometry gives

$$A(v,t) = k\left(\frac{S^2}{2\omega R} - \frac{\omega R^3}{v^2}\right); \quad \frac{2\omega R^2}{S} \leq v \leq \infty .$$

This is then used to obtain the correction

$$f(x) = \frac{A(v,t)}{A(v_\infty,t)}$$

$$= 1 - \frac{2\omega^2 R^4}{S^2 v^2} ; \quad \frac{2\omega R^2}{S} \leq v \leq \infty .$$

For neutrons having velocities between the cutoff velocity and twice this velocity it can be shown by similar geometric inspection that $f(x) = 2\left[1 - \frac{2\omega R^2}{Sv} + \frac{\omega^2 R^4}{S^2 v^2}\right]$

$$f(x) = \frac{2\omega R^2}{Sv}\left(1 - \frac{\omega R^2}{Sv}\right) \; ; \; \frac{\omega R^2}{S} \leq v \leq \frac{2\omega R^2}{S} \; .$$

These correction functions permit the relating of the measured spectrum back to the incident spectrum. The results from the initial operation of the slow neutron chopper presented later utilize the above correction functions.

Another factor involved in the operation of a chopper is the resolution. This is a term which is used to define the velocity range in a counting channel, or to define the probability of recording a certain velocity neutron by the time of flight technique. The resolution function actually should include the length of the neutron burst, the counting gate time width, the neutron path in the detector, and the errors introduced in time for detector response. The convolution of the time base curves for these factors results in a curve called the resolution function. The time width of the resolution function at half height is the error in time, Δt, which is used to define the chopper resolution. The resolution is then defined as

$$R = \frac{\Delta t}{D} \; ,$$

which will give the velocity range in a channel. Rather than convolute curves of unknown quantities, the resolution for this instrument is calculated by using the empirical equation given in reference (9) where

$$R = \left(\frac{t_f}{D} \right)^2 v \ (10^{-6}) \ ,$$

where t_f is the time of flight of the mean velocity neutron in a channel, and D is the flight length.

Experimental measurement of resolution and refinements in the aperture function corrections, to include the range of neutron velocities in a counting channel, are discussed in the conclusions.

DESIGN OF THE CHOPPER

The design of the slow neutron chopper incorporates features that provide the various theoretical functions. It is desirable to design these features to allow variations in as many parameters as possible. This can be done only to the extent that a safe and functional design is not compromised.

A slow neutron chopper is normally considered for operation in the neutron energy region of a few thousandths of an electron volt to perhaps a few tenths of an electron volt. The parameters that affect the energy range in operation are the rotational speed of the chopper, the thickness of the transmission slits in the rotor and the slit length. Most previous designs have allowed variation of the rotational speed as the only factor to affect the energy range. A variation of the slit thickness coupled with the changes in rotational speed increases the flexibility of the chopper.

Combining some practical requirements for the design with the operational requirements produces a set of conditions that can be used to outline the design of this chopper. For practical reasons, the rotational speed of the chopper must be limited to allow the use of commercially available bearings and drive motors. Also, the materials used in fabrication

should be readily available and easily worked with standard shop practices. For rigid speed control it is desirable to use a synchronous motor drive.

The limiting factors in the energy range of operation are the cutoff velocity as the minimum, and the effective black body absorption of neutrons as the maximum. The combination of speed and slit dimensions define the cutoff velocity from the equation

$$v_{co} = \frac{\omega_R 2}{S} .$$

The black body absorption of neutrons requires a material with a high absorption cross section. Cadmium is a readily available material that provides a neutron absorption cross section greater than 1000 barns up to energies of about 0.3 ev. (5). Other absorbing materials will be discussed in the conclusions. The equation taken from the text by Glasstone and Edlund (3) for the transmission of neutrons, I/I_o, by an absorbing material is

$$\frac{I}{I_o} = e^{-N\sigma x}$$

where N is the number of nuclei per cubic centimeter, σ is the neutron absorption cross section of the material in square centimeters and x is the thickness of the material in centimeters. The value of N is calculated from

$$N = \frac{\rho N_o}{A}$$

where ρ is the density, A is the atomic weight and N_o is Avogadro's Number. The value of N for cadmium is 0.046×10^{24} atoms per cubic centimeter. Using this value for N and a neutron absorption cross section of 1000 barns, the fraction of an incident beam of neutrons transmitted through a thickness of 0.07 cm of cadmium is

$$\frac{I}{I_o} = 0.038 \ .$$

This value shows that a thickness of 0.07 cm of cadmium will transmit less than 4% of the incident neutron beam up to energies of 0.3 ev, and will provide a suitable absorber plate material for this design.

The flight path most readily available at the reactors at this University is less than ten meters. To prevent overlapping of the neutron pulses generated by the chopper, the detector should be located close enough to the chopper to permit the slowest neutron in a pulse to arrive at the detector before the fastest neutron in the next pulse arrives. Assuming that the fastest neutron can have an infinite velocity and the slowest neutron in a pulse is at the cutoff velocity, the geometric relation between distance, D, and

time of flight gives

$$D \leq \frac{\pi R^2}{S} .$$

Incorporating these factors into a design for the chopper results in the following tentative features which are based on a variable speed drive and a moveable carrier for the sandwich assembly.

$\omega \leq 15{,}000$ rpm

$S \leq 0.020$ ins.

$R = 1.5$ ins.

$D \leq 10$ meters

$E_{c.o.} \leq 0.3$ ev

The detailed drawings of the design which incorporates these features are shown by drawings on file at Ames Laboratory. An artist's concept of this design is shown in Figure 5. The design has the unique feature of permitting easy replacement of the sandwich assembly. This readily allows the absorber material to be changed or the slit thickness to be changed. It is very easy to increase the slit thickness by rotating the sandwich carrier assembly through an angle α. The effective slit thickness is then

$$S_{eff} = \frac{S \text{ min.}}{\cos \alpha} .$$

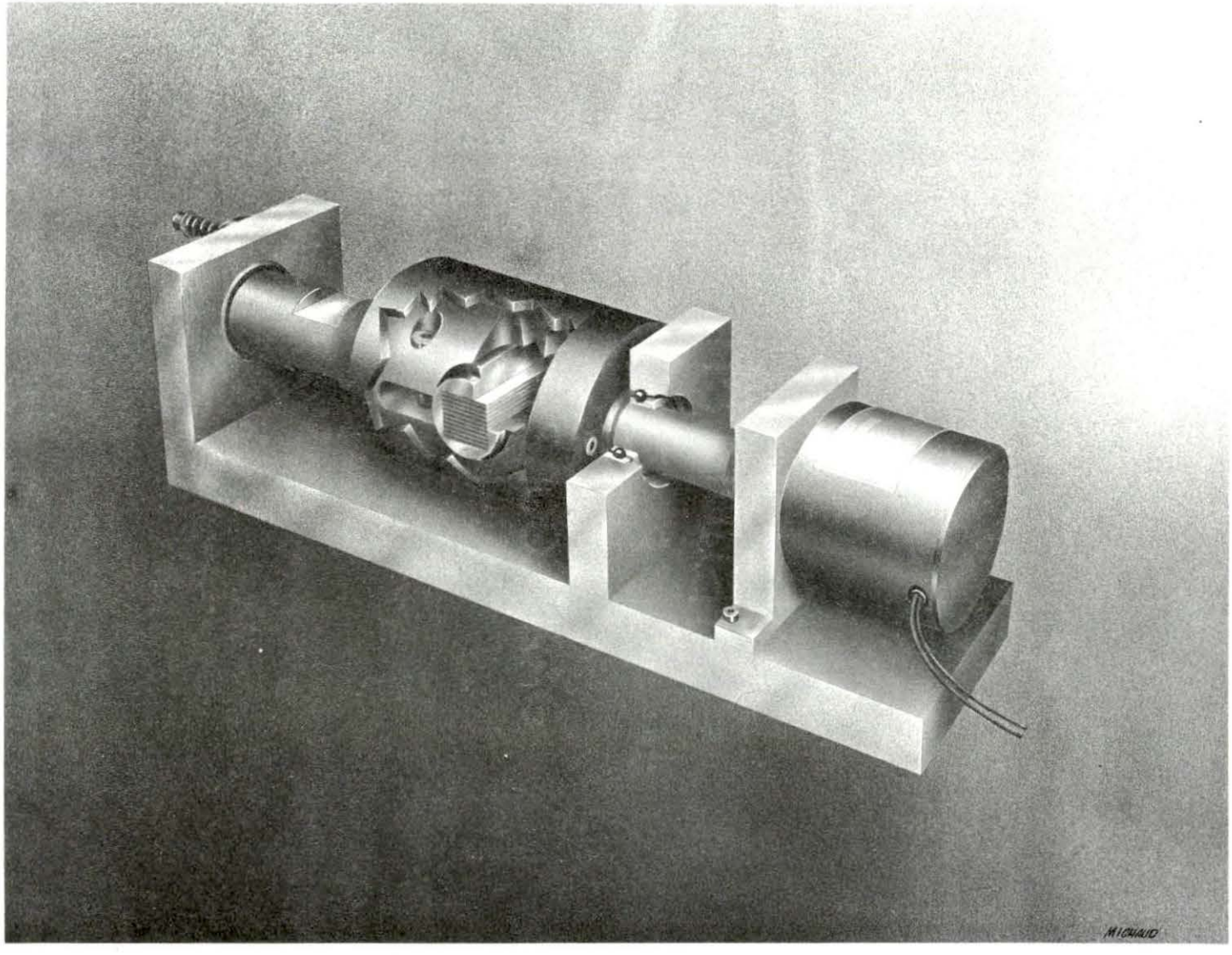

Figure 5. Artist's concept of chopper

The variable speed drive for the chopper is provided by a hysteresis wound synchronous motor. This type of motor permits variation of input frequencies and will run at synchronous speeds with a rather large deviation in the frequency. The chopper is designed to readily accept a 2 pole, 60 cycle motor or a 4 pole, 400 cycle motor. By varying the frequencies to both sides of the nameplate ratings, these two motors can provide synchronous speeds from 3,000 to 15,000 rpm. A variable frequency input to a power amplifier provides a driving source for these motors.

Figure 5 shows the basic unit frame supporting two super precision bearings which carry the rotor. The rotor is sectioned to show the cross mounting of the sandwich carrier which is held rigidly in place by compression of the rotor. This assembly is encased in an aluminum shell to provide a containing cover with a minimum of wind drag during high speed rotation. The drive motor is mounted directly to the main rotor shaft to eliminate drive error. Two polished flats on the rotor shaft are used to reflect a light beam twice per revolution onto a photodiode. This provides an electric signal in direct relation to slit position which is used to start the counting circuits. The electronics used in the motor drive

and the counting circuits were not designed by this author.

Prior to the fabrication of the chopper, its ultimate safety was analyzed. The possibility of the moveable sandwich carrier changing position during operation is considered the most serious danger. The chopper was designed to insure rotor balance and holes and bolts were placed to provide dynamic balance at all times. The compression of the rotor has a clamping effect on the sandwich carrier which holds it in place in the rotor during operation. This clamping pressure has been estimated by calculations to be on the order of several hundred pounds.

The final containment of the sandwich assembly is the aluminum shell. Using the equations for stress in rotating cylinders from Roark (8) the stress in this shell can be calculated. The radial inertial stress was calculated and is negligible in this shell. The equation for the maximum tangential stress is

$$\text{Max } s_t = \tfrac{1}{4} \frac{\rho \omega^2}{386.4} \left[(3 + \nu) R_i^2 + (1 - \nu) R_o^2 \right]$$

where ρ is density, ω is rotational speed, R_i is the inner radius, R_o is the outer radius, and ν is Poisson's ratio. Using the appropriate values for this design gives a maximum tangential stress of 1,850 psi. The notched section of the

shell which accepts the flat face of the sandwich carrier will show a stress concentration point. The above stress is a tangential stress in the shell, and a stress concentration factor of three or four would be possible but not probable. Even this stress would be less than 10,000 psi which is certainly less than the safe working stress of about 25,000 psi for this aluminum alloy.

By assuming distortion of the aluminum shell and subsequent displacement of the sandwich carrier, the shear stress in the shell can be estimated. The amount of displacement must be assumed, and unless the shell is ruptured it cannot allow a displacement of more than a few thousandths of an inch. By assuming a displacement of 0.010 inch, and calculating the force exerted by the unbalance in the carrier results in a shear stress to the shell of 10,700 psi. This again is within the safe working stress for the aluminum shell.

The chopper was run at operational speeds with no difficulty.

FABRICATION AND INITIAL OPERATION

The slow neutron chopper was fabricated in the machine shop at the Ames Laboratory Research Reactor facility. The parts were fabricated in a sequence that allowed a very close fit between mating parts. The significant techniques will be discussed here to permit at least the proper replacement of the slit assembly.

The base for the chopper was machined first, followed by the machining of the rotor. The cross hole in the rotor was bored to size and the boring was stopped when the diameter was within tolerances and a smooth finish was obtained. This diameter was then used as the reference for the outside diameter of the slit assembly.

The carrier for the sheets of cadmium and aluminum was not fabricated until the stack up of the sheets was completed. The machining of the alternating sheets of cadmium and aluminum was done with a clamp of aluminum stock holding them in compression. The height of the stacked assembly of sheets thus could be determined and used in machining the carrier. The carrier was machined to fit the assembly of sheets, and the outside diameter of the carrier was kept oversize until the assembly was bolted together. Then the outside diameter

was turned down until it was less than a thousandth of an inch smaller than the bore in the rotor. This small difference in diameters permitted the easy clamping of the carrier by the bolts in the rotor. The length of the assembled carrier was machined to match the outside diameter of the rotor and the aluminum covers were fabricated. The entire assembly was checked at low speeds for lack of balance. The design and careful machining proved to provide good balance and vibration was not ascertained at any speed. The chopper subsequently has been operated as it was first assembled.

The initial operation of the chopper was planned to obtain experience in operation and counting techniques. The data obtained gives the spectrum of thermal neutrons in the thermal column of the Ames Laboratory Research Reactor and is intended to prove the validity of the design concept and operational technique. The experience gained can be employed later to gather very useful data. With this plan in mind, the initial operation of the chopper was scheduled for as simple an operation as possible, consistent with obtaining the data required to define a velocity spectrum.

The thermal column at the Research Reactor provided a thermalized beam of neutrons for the initial operation. An

available collimating plug at the thermal column permitted about a one-half inch diameter beam of thermal neutrons to be incident on the chopper. To provide as wide an energy range as possible and for ease of initial operation, the 3600 rpm drive motor was used from the standard 60 cycle AC line to provide a constant slow speed drive. The counting circuitry was assembled using a spare detector and amplifier available in the Reactor Division. The detector, a BF_3 chamber, was placed in a cadmium sheath, four feet long, to provide collimation in front of the detector. A preset timer and scaler were used to complete the counting circuit. The starting trigger for the scaler was generated by an oscilloscope modifying the trigger signal obtained from the photodiode. A block diagram of the system used for this initial operation is shown in Figure 6. A replica of the dual trace displayed on the oscilloscope showing the trigger signal from the photodiode and the delayed gate time for control of the scaler is shown in Figure 7.

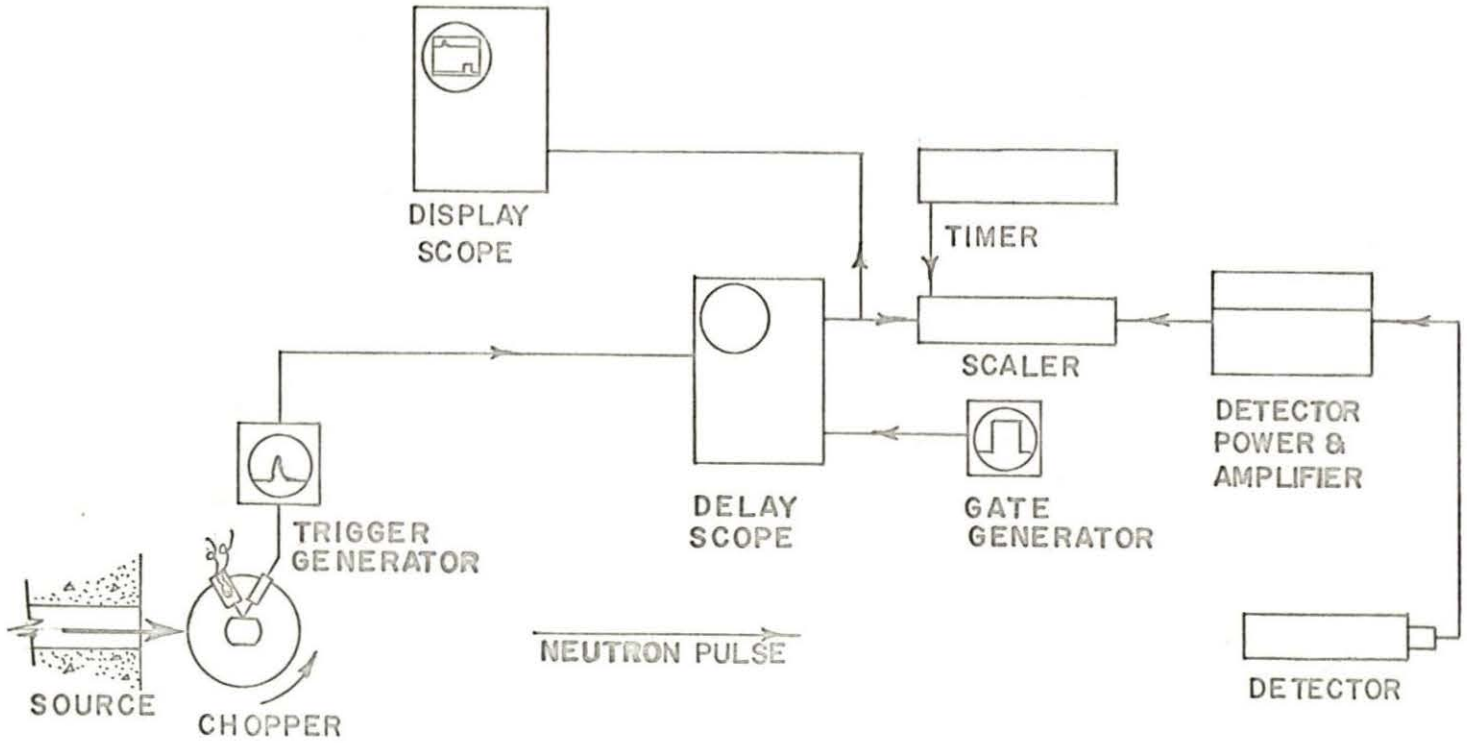

Figure 6. Block diagram of initial setup

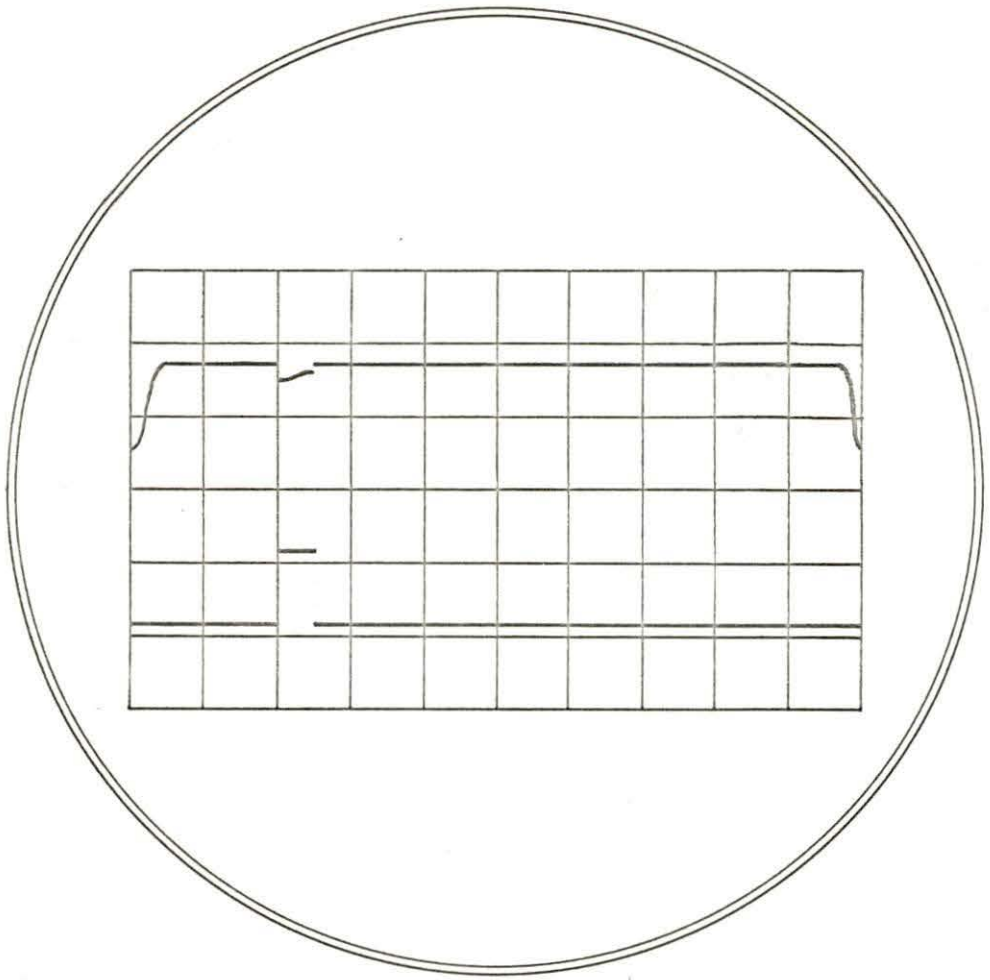

Figure 7. Scope trace

RESULTS OF OPERATION

The slow neutron chopper was set up at the reactor thermal column with the following conditions set for the operation. The aluminum slits were set parallel to the rotor axis to provide a slit width of 0.020 inch. The drive motor provided a synchronous rotational speed of 3600 rpm. The photodiode trigger was adjusted to provide a 2 volt signal at 2 degrees ahead of the shutter fully opened position. The detector was located at a flight length of less than 8.9 meters to avoid overlap of the pulses. The preliminary counting indicated the counting rate was quite low at the longer flight lengths, so the detector was located at a distance of 13 feet 4 inches, 4.06 meters, from the chopper centerline to the detector center. The reactor was operated at a 5 megawatt thermal power level for all counting.

The counting circuitry was assembled to record counts from the collimated BF_3 detector in a scaler. The trigger signal from the chopper was detected by an oscilloscope which then delayed this signal with the adjustable internal delay circuit. The delayed trigger then opened the counting gate which was set at one-twentieth the duration between trigger pulses. Thus at 3600 rpm, the time between trigger pulses

was 8.33 milliseconds and the counting gate time was 0.417 milliseconds. This provided a maximum of 20 channels of information for the entire energy range from cutoff to infinite velocity neutrons. The cutoff velocity for the settings of the chopper during this operation was 1,070 meters per second, which corresponds to an energy of 5.9×10^{-3} ev. Due to the detector location, the cutoff velocity occurred after the ninth counting channel.

Prior to recording the data shown in Table 1, the chopper was operated with the counting gate circuit open. This permitted the scaler to record all the neutrons transmitted by the chopper. Three successive ten minute runs were made to provide a basis for count variation statistics. In addition to these open gate runs, the beam hole was covered with cadmium and a 10 minute background count was made with the counting gate open. These counts are shown below and are used for variation and background corrections in Table 1.

Run 1-553 counts/10 min.

Run 2-516 counts/10 min.

Run 3-534 counts/10 min.

Background Run-66 counts/10 min.

On the basis of these counts, the variation in counting

rate is calculated as

$$\pm \frac{18 \text{ counts}}{534 \text{ avg. counts}} = \pm 3.4\% \ .$$

This is the average deviation in the counting rate. The background counts are based on a counting time of 10 minutes. It is assumed that the background counts for 20 minutes would be a total of 132 counts. Inasmuch as the counting gate was set for one-twentieth the duration between pulses to provide 20 counting channels, the background count correction in Table 1 is 6.6 counts per channel. This correction is applied to give the nearest integer in counts per channel. The background rate is calculated this way to eliminate the uncertainty in gate timing which was known only from a visual display on the oscilloscope. This also eliminates the error in dead time resulting from gate actuation. The correction based on total estimated background counts is justified by the counts in the channels beyond the cutoff velocity.

The ratio of background counts to total counts is

$$\frac{66}{534} = 0.12$$

which should provide sufficient accuracy in the recorded counts per channel.

Table 1 then shows the actual counts recorded in the

Table 1. Data from initial operation

Channel	Counts/ 20 min.	Counts- background	t_{mean} of arrival	$v_{mean} = \frac{D}{t_m}$ *	f(x)	Corrected counts
1	11	5	0.2083 msec.	19,150 m/sec.	0.994	5.05
2	16	10	.6249	6,410	.944	10.6
2 1/2	44	38	.8333	4,800	.901	42.2
3	302	296	1.0416	3,840	.845	350
3 1/2	418	412	1.2497	3,200	.778	530
4	434	428	1.4583	2,745	.698	613
4 1/2	328	322	1.6667	2,400	.604	534
5	204	198	1.8750	2,135	.500	396
6	77	71	2.2916	1,745	.476	149
7	25	19	2.7083	1,475	.400	47.5
8	12	6	3.1254	1,280	.276	21.8
9	7	1	3.5425	1,130	.104	9.6
10	7	1	3.9592	(1,010)		
11	6	0	4.3758	(915)		
12	7	1	4.7924	(835)		

*v_{mean} shown in ( ) are less than v_{co}.

counting channels. The gate was moved by visual observation on the scope to the midway point between channels when the count rate from one channel to the next showed large variations. These counts denoted by 1/2 channels are presented to provide better resolution of the spectrum. Table 1 also shows the corrected counts after the background counts have been subtracted from the recorded counts. The mean time of arrival of the neutrons in a channel is based on the midpoint time of the counting gate for that channel. This mean time of arrival is then used to calculate the mean neutron velocity of the neutrons counted in the channel. These values are used in computing the aperture function correction, f(x), as defined earlier in this thesis. The final tabulation in Table 1 is the corrected count rate for a channel which is then used in plotting the spectrum incident on the neutron chopper according to the function defined earlier. The spectrum incident on the chopper is shown in Figure 8 along with a standard Maxwell-Boltzman spectrum taken from Kaplan (6).

The most probable velocity for the measured spectrum is 2,750 meters per second. Using this velocity in the equation for the relation between most probable velocity and temperature gives a spectrum temperature of

$$T = 458^{\circ}K \text{ or } 185^{\circ}C.$$

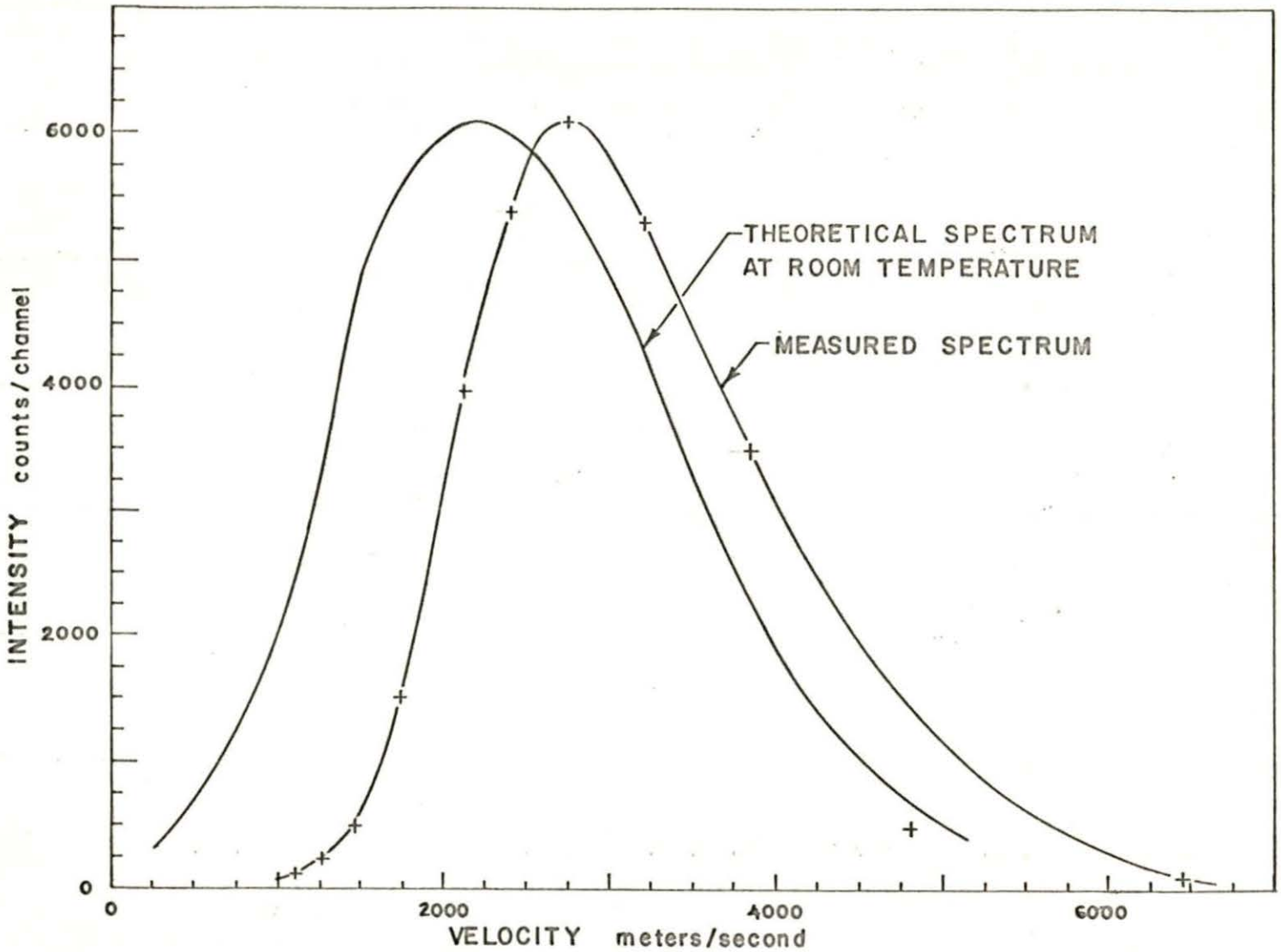

Figure 8. Spectrum curve

This temperature describes the measured spectrum. The temperature of the graphite in the thermal column measured by a thermocouple during operation was 46°C. A difference between these temperatures is commonly found and reported by others (3,6).

The resolution of the measurements shown graphically in Figure 8 can be calculated from the equation given in the section on discussion of theory. The resolution for the most probable velocity is then found from

$$R = \left(\frac{t_f}{D}\right)^2 v \ (10^{-6}).$$

The values for this velocity, taken from Table 1, then give the resolution as 756 microseconds per meter. This would correspond to a neutron velocity of 1,320 meters per second or an energy of about 0.009 ev.

SUMMARY AND CONCLUSIONS

The results obtained in the initial operation of the chopper are presented to show the validity of the design and operational techniques. To this extent, the results shown in Figure 8 provide support for the belief that the design objective has been fulfilled. It was not the intent of the author to develop counting techniques for use with the chopper, and as a consequence the method of counting used in the initial operation is not an optimum counting system.

The basic fault in the counting circuit is the inability to obtain a sufficient number of counting channels. It is desirable to have as many counting channels as possible to offer the best definition of the mean neutron velocity in a channel. The method of computing the neutron velocity as the velocity corresponding to the mean time of flight for a channel has an inherent error. This error arises from the presence of a range of neutron velocities counted per channel. The more this range can be minimized by increasing the number of counting channels, the better the results will be. The resolution will be improved in the measurements as the channel gate time is shortened.

A new counting circuit is being developed to obtain more

counting channels when using the slow neutron chopper. The new circuit will incorporate a 400 channel analyzer to provide a sufficient number of channels to store neutron counts and give much better resolution in future operation.

The counting rate was rather low for the initial operation. This was caused by two factors, the small neutron beam and the small detector. The neutron beam size incident on the shutter can be increased from about one-half inch to one inch diameter increasing the transmission by a factor of about four. The small detector can be replaced by a larger array of detectors which will cover the area of the slightly diverging beam. Measurements made with a hand held survey meter indicated that an increase of about a factor of six can be obtained in the counting rate if the entire beam is counted. These two factors can raise the counting rate significantly and allow the extension of the flight path to the length which just precludes the overlap of neutron pulses.

With the expansion of the counting circuitry as outlined, the measurements should provide very good resolution. An experimental verification of the resolution of a slow neutron chopper is described by Egelstaff (1). This method involves the measurement of the neutron transmission of iron powder

and plotting the neutron wavelength versus neutron transmission. A sharp break should occur in transmission corresponding to a wavelength of twice the lattice spacing in the 110 planes of α-iron. The sharpness of the break in the plotted transmission is a measure of the resolution of the chopper.

Another improvement which could be made in this slow neutron chopper is the installation of different absorbing material in the shutter. Other experimenters have used nickel for absorber plates. Nickel has a rather low absorption cross section for low energy neutrons, but it exhibits a wide range with a uniform cross section. This author believes that a selection of rare earth elements will provide a superior absorber material to others used in the past. An inspection of cross section curves published by Brookhaven National Laboratory (5) shows that several rare earth elements have large absorption cross sections up to about 10 ev. Although these elements have anti-resonance regions of low cross sections at certain energies, an alloy could be developed for use as the absorber material to extend the operating range of the chopper from thermal neutrons to neutrons having energies as high as 10 ev. An alloy of europium, gadolinium and samarium should provide an effective cross section of nearly 1000 barns or

more for the range of 0.001 to 10 ev. A composite graph of the cross sections of these elements, as well as others, will be made in an effort to select an absorber material for extending the energy range of the chopper.

The extension of the counting circuitry and subsequent improvement in resolution also will permit more refined corrections in the aperture function described in this paper. The aperture function can be delayed to include the time elapsed during time of flight of the neutrons to the detector. A function can be developed which will describe the arrival of neutrons at the detector dependent on time and velocity. The counting rate indicated by the counts per channel and the channel gate time can then be corrected by defining a function describing the spectrum incident on the shutter in terms of the new delayed aperture function. The inherent error produced by the range of neutron velocities in a counting channel can be minimized also by defining the counting rate in a channel by linear interpolation between channels. The counting rate in a channel then can be corrected by computing a value and comparing it to the measured value. The difference in this comparison can be used to provide the correction, and this can be repeated until the spectrum converges to the inci-

dent spectrum. These refinements are small in magnitude, but with good resolution in the measurements they should be made to provide correct results.

After many of these improvements are made, the neutron chopper will be used to measure the neutron energy spectrum in greater detail. It is also expected that this instrument will be used in the future in the measurement of cross sections of different materials. A request to measure the neutron energy spectrum after diffraction by a monochromating crystal in a neutron diffractometer should result in another application for this neutron chopper. The instrument should provide a useful research tool for future programs at the reactor facilities in this area.

LITERATURE CITED

1. Egelstaff, P. A. The operation of a thermal neutron time of flight spectrometer. Journal of Nuclear Energy 1: 57-75. 1954.

2. Fermi, E., Marshall, J. and Marshall, L. Thermal neutron velocity selector and its application to the measurement of the cross section of boron. Physical Review 72: 193-196. 1947.

3. Glasstone, Samuel and Edlund, Milton C. The elements of nuclear reactor theory. Princeton, N.J., D. Van Nostrand Co., Inc. 1952.

4. Hoch, R. J. Analysis of a neutron chopper to be used with the HTLTR. U.S. Atomic Energy Commission Report HW-80020 [Hanford Atomic Products Operation, Richland, Washington]. 1963.

5. Hughes, Donald J. and Schwartz, Robert B. Neutron cross sections. U.S. Atomic Energy Commission Report BNL-325 [Brookhaven National Laboratory, Upton, N.Y.]. 1958.

6. Kaplan, Irving. Nuclear physics. 2nd ed. Reading, Mass., Addison-Wesley Publishing Co., Inc. 1963.

7. Mastovoi, V. I., Pevzner, M. I. and Tsitovich, A. P. A mechanical neutron velocity selector. International Conference on the Peaceful Uses of Atomic Energy Proceedings 1955: 12-21. 1956.

8. Roark, Raymond J. Formulas for stress and strain. 3rd ed. New York, N.Y., McGraw-Hill Book Co., Inc. 1954.

9. U.S. Atomic Energy Commission. Argonne National Laboratory. Fermi slow neutron chopper and its applications: training reactor laboratory experiment [manual]. Argonne, Ill., author. ca. 1962.

ACKNOWLEDGMENTS

I wish to thank Dr. Danofsky for suggesting this thesis topic and for his counseling and guidance. I also express my sincere gratitude to members of the Ames Laboratory Reactor Division for their assistance in machining, electronics, art work and reactor operation.